Use of a corrected standardized uptake value based on the lesion size on CT permits accurate characterization of lung nodules on FDG-PET

Marc Hickeson, Mijin Yun, Alexander Matthies, Hongming Zhuang, Lars-Eric Adam, Lester Lacorte, Abass Alavi

Division of Nuclear Medicine, Department of Radiology, 110 Donner Building, Hospital of the University of Pennsylvania, 3400 Spruce St., Philadelphia, PA 19104, USA

Received 28 April and in revised form 25 May 2002 / Published online: 2 October 2002

Abstract. The purpose of this study was to determine the actual standardized uptake value (SUV) by using the lesion size from computer tomography (CT) scan to correct for resolution and partial volume effects in positron emission tomography (PET) imaging. This retrospective study included 47 patients with lung lesions seen on CT scan whose diagnoses were confirmed by biopsy or by follow up CT scan when the PET result was considered negative for malignancy. Each lesion's FDG uptake was quantified by the SUV using two methods: by measuring the maximum voxel SUV (maxSUV) and by using the lesion's size on CT to calculate the actual SUV (corSUV). Among small lesions (2.0 cm or smaller on CT scan), ten were benign and 17 were malignant. The average maxSUV was 1.43±0.77 and 3.02±1.74 for benign and malignant lesions respectively. When using an SUV of 2.0 as the cutoff to differentiate benignity and malignancy, the sensitivity, specificity, and accuracy were 65%, 70%, and 67% respectively. When an SUV of 2.5 was used for cutoff, the sensitivity, specificity, and accuracy were 47%, 80%, and 59% respectively. The average corSUV was 1.65±1.09 and 5.28±2.71 for benign and malignant lesions respectively. Whether an SUV of either 2.0 or 2.5 was used for cutoff, the sensitivity, specificity, and accuracy remained 94%, 70%, and 85% respectively. The only malignant lesion that was falsely considered benign with both methods was a bronchioalveolar carcinoma which did not reveal any elevated uptake of fluorine-18 fluorodeoxyglucose (FDG). Of the large lesions (more than 2.0 cm and less than 6.0 cm), one was benign and 19 were malignant and the corSUV technique did not significantly change the accuracy. It is concluded that measuring the SUV by using the CT size to correct for resolution and partial volume effects offers potential value in differentiating malignant from benign lesions in this population. This approach appears to improve the accuracy of FDG-PET for optimal characterization of small lung nodules.

Keywords: Lung nodule – Fluorodeoxyglucose – PET – Diagnosis – Standardized uptake value

Eur J Nucl Med (2002) 29:1639–1647
DOI 10.1007/s00259-002-0924-0

Abass Alavi (✉)
Division of Nuclear Medicine, Department of Radiology,
110 Donner Building, Hospital of the University of Pennsylvania,
3400 Spruce St., Philadelphia, PA 19104, USA
e-mail: alavi@rad.upenn.edu
Tel.: +1-215-6623069, Fax: +1-215-6623049

Introduction

Carcinoma of the lung is the leading cause of cancer death among men and women in the United States and many other countries. Approximately 130,000 new solitary lung nodules are identified each year in the United States. More than 40% of noncalcified solitary lung nodules seen on the chest X-ray are benign. Computer tomography (CT) scan has played a major role in characterizing these lesions during the past two decades. However, the classic criteria for benignity are infrequently seen, leaving a significant number of indeterminate lesions on CT. If the nodule is not definitely benign by its characteristics on CT, then further investigation is required [1].

Fluorine-18 fluorodeoxyglucose (FDG) positron emission tomography (PET) has been proven to be of value in characterizing the nature of the lesion by measuring its metabolic activity. Malignant cells actively metabolize glucose and, consequently, appear active on FDG images. The FDG-PET scans can be interpreted qualitatively or semi-quantitatively and both approaches have been employed to determine the degree of metabolic activity in the lesion. Qualitative evaluation of lung lesions on attenuation-corrected images (e.g., visual analysis) is based upon comparison of the intensity of uptake in the lesion with

normal mediastinal activity; if the intensity of uptake is higher than that in the mediastinum, malignancy is suspected [2]. Semiquantitative determination of FDG activity of the lesion is accomplished by calculating the standardized uptake value (SUV) [2, 3] or the lesion to background ratio. The SUV, an index of glucose metabolism on FDG-PET images, represents the amount of uptake in a given region of interest (ROI) in relation to the average uptake throughout the body. FDG-PET by visual analysis has been reported to have slightly higher sensitivity but lower specificity as compared with SUV measurement [4]. Qualitative evaluation of the lesion offers a more objective reporting of the uptake of the lesion [5]. The SUV threshold used by most investigators to differentiate benignity from malignancy in lung lesions is 2.5 [3, 6, 7, 8], above which the lesion is considered to be malignant:

$$\mathrm{SUV} = \frac{\mathrm{MeanROIactivity(MBq/ml)}}{\mathrm{Injecteddose(MBq)/Bodyweight(g)}} \times \frac{1}{\mathrm{decayfactorof}^{18}\mathrm{F}} \quad (1)$$

(The above equation is from reference [3].)

The spatial resolution of the PET systems varies significantly and is typically between 5 and 10 mm for clinical scans. This is significantly worse than the best possible spatial resolution, which is measured under ideal conditions and used by manufacturers. The degradation of spatial resolution is due to changes in sampling and filtering, scattered and random events, and respiratory motion. The contrast between tumor and normal lung decreases as the size of the lesion becomes smaller and may disappear beyond a certain point [9]. This may result in false negative results using either qualitative or SUV criteria for small lesions (<1.5 cm) because of the partial volume averaging effects due to the limited resolution of the system [6]. We have adopted a new method to correct for the resolution effect in which the real size on CT scan is used as the basis to calculate the SUV (Fig. 1). The accuracy of this method was compared with of the conventional approach for calculating SUV for small (equal to or less than 2.0 cm in maximal diameter on CT scan) and for large lung lesions (more than 2.0 cm and less than 6.0 cm in maximal diameter on CT scan).

Fig. 1. A The profile of a small lung nodule with uniform FDG uptake using an "ideal" PET scanner with a perfect spatial resolution; the lung itself shows uniformly low FDG activity. **B** The profile of perceived FDG activity with our current PET scanners through the same nodule in the same lung is indicated by the *thick-lined curve*. The true distribution of FDG (ideal profile) is indicated by the *broken line*. The *thin line* indicates the profile of perceived FDG activity from the lung nodule and the *dotted line* indicates that from the uninvolved adjacent lung parenchyma (background). Note that the area under the profile using the "ideal" PET scanner indicated in **A** is equal to that using the current PET scanner indicated in **B**

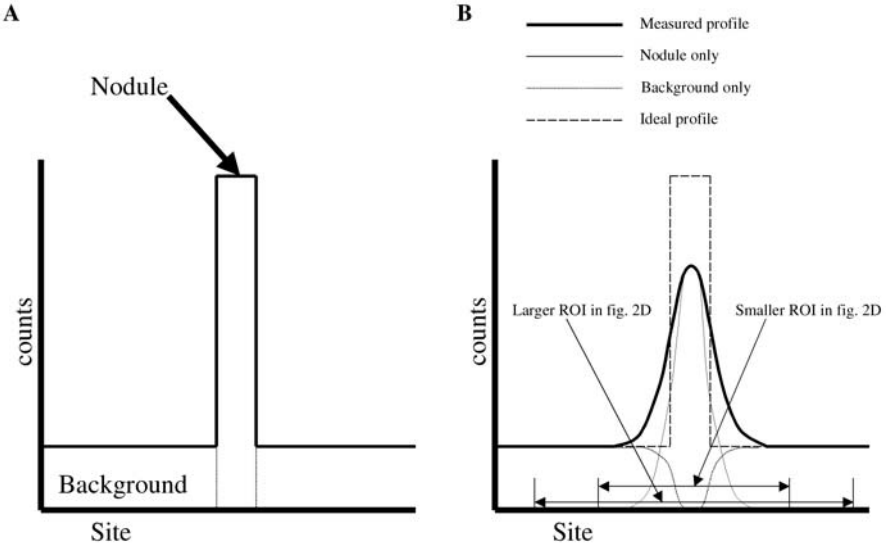

Materials and methods

Patient population. This retrospective study included 47 patients (age range 31–84 years; mean 66.6 years). All patients were referred for the evaluation of a lung lesion of known size as determined on CT of the thorax performed within 45 days of the FDG-PET scan or by serial CT scans done before and after the FDG-PET scan demonstrating stability of size. All malignant lesions examined were eventually confirmed by histology. Lung lesions were subdivided into two categories: small lesions (equal to or less than 2.0 cm in maximal diameter on CT scan) and large lesions (more than 2.0 cm but less than 6.0 cm in maximal diameter on CT scan). All benign lesions were confirmed either by excisional biopsy or by serial CT scans demonstrating stability of lesion size for at least 24 months or a spontaneous decrease in lesion size. All patients in this category were free of any malignancy on clinical follow-up during that period of time. None of the patients received chemotherapy or radiation therapy within 1 month of the PET study or after the biopsy if performed prior to the PET study.

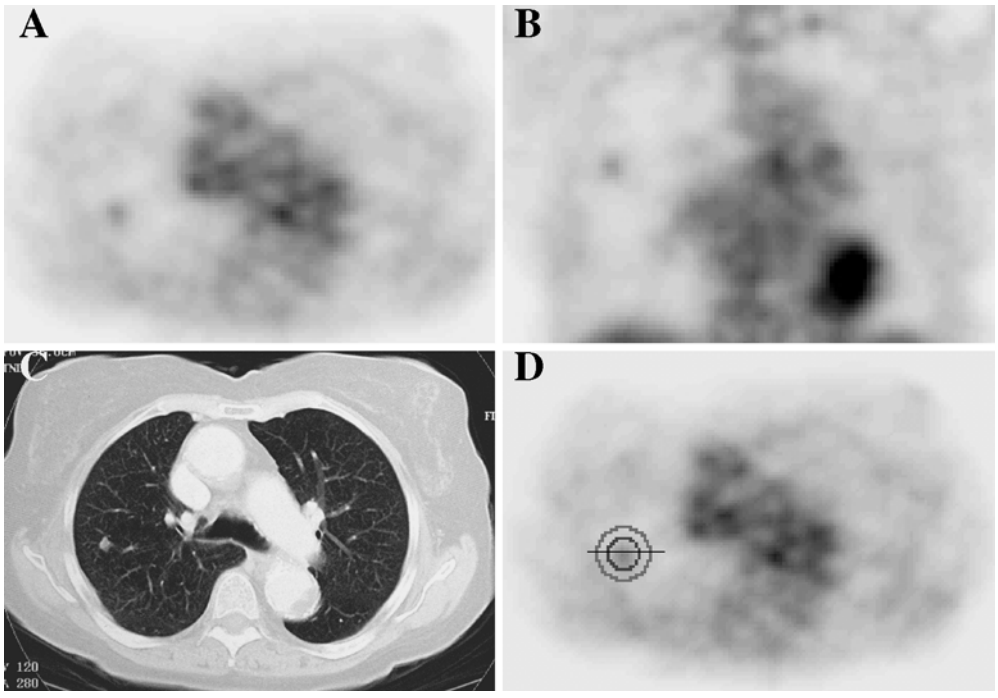

Fig. 2A–D. Images of a 72-year-old female (patient no. 4) with a small cell lung carcinoma. The transverse image (**A**) and coronal image (**B**) of the FDG-PET scan demonstrated a focus of mildly increased uptake in the right middle lobe. The chest CT image demonstrates that the nodule measures 1.0×0.8 cm (**C**). The maxSUV was 1.39, which is less than the threshold for malignancy. **D** The corSUV was obtained by drawing an ellipsoid or circular ROI (*in black*) with a diameter of 0.8 cm (two voxels) larger than that of the area of perceived increase in activity at the plane of maximal FDG uptake and drawing another ROI (*in gray*) with a diameter of 0.8 cm larger than the first to determine background activity (activity per volume outside the smaller ROI and inside the larger ROI). The corSUV was then obtained by determining the activity in the first smaller ROI corrected background activity, dividing by the lesion's size on CT and the ratio of the injected dose to the body mass and correcting for decay of ^{18}F (see Eq. 2). The corSUV of this lesion was 3.54, which exceeds the threshold for malignancy. The *horizontal line* through the nodule approximates the profile in Fig. 1B.

FDG-PET imaging procedure. PET scans were performed using a whole-body CPET scanner (ADAC/UGM, Philadelphia, Pa.). The patient fasted for at least 4 h before receiving the injection. The images were acquired approximately 60 min after the administration of 2.5 MBq (0.068 mCi) of FDG per kilogram of body weight. The images were reconstructed using the RAMLA iteration reconstruction algorithm [10, 11] and were attenuation corrected by using an external source of cesium-137. Only the fully corrected images were used for this investigation. The reconstructed images had a slice thickness of 4 mm.

CT scan. The lesion size was determined by measuring the diameter in two perpendicular axes in the transaxial plane in which the lesion appeared the largest in surface area if the scan was available for analysis or by accepting the report by the radiologist who interpreted the CT scan if the study was performed in an outside institution.

FDG-PET image interpretation. The lesions were independently identified from the CT scan and every effort was made to match the corresponding images of these two modalities for the purposes of this analysis. Each lesion's SUV was determined by using two different methods. The maximum voxel SUV (maxSUV) was determined in a circular ROI with a diameter of 0.8 cm (two voxels) at the plane with maximal FDG uptake of the lesion. The size of all ROIs was determined by the sum of the fractions of all voxels occupied by the ROIs. The maxSUV was calculated by determining the mean FDG activity of a voxel within this small ROI and using the formula shown in Eq. 1.

In the second method, the SUV was corrected for underestimation of true metabolic activity of the entire lesion due to the resolution and partial volume effects (corSUV). Two circular or ellipsoid ROIs were drawn around the lesion. The smaller of them included all the voxels associated with the lesion. In practice, the regions were drawn 0.8 cm (two voxels) outside the 50% uptake level of the lesion (see smaller ROI in Fig. 2D). The second larger ROI included the smaller ROI as well as its surrounding background (see larger ROI in Fig. 2D). Thus, the lesion background could be determined from the average uptake outside the smaller ROI and inside the larger ROI. Note that the halfway point between the maximum lesion activity and surrounding background activity is frequently used as the true size of the lesion. The background uptake was then subtracted from the average uptake in the small ROI. Therefore, the corSUV was calculated by including the injected dose, patient's weight and time after injection and using the following formula:

$$\mathrm{corSUV} = \frac{\frac{\mathrm{region's activity(MBq)} - \mathrm{background activity(MBq)}}{\mathrm{lesion's size on CT scan(cm^3)}}}{\frac{\mathrm{injected dose(MBq)}}{\mathrm{patient's weight(g)}}} \quad (2)$$

where background activity = activity/volume in background × (region's volume – lesion's size on CT scan in cm^3). Note that the volumes of the ROIs are obtained by multiplying the surface area of the ROIs by 0.4 cm, the slice thickness of the FDG-PET images. This system is calibrated using a 30-cm uniform cylindrical

Table 1. Standardized uptake values and characteristics of lung lesions

Patient no.	Site of lesion	Lesion size on CT (cm)	maxSUV	corSUV	Characteristics of lesion
1	RUL	1.8×1.2	1.43	1.83	Stable on CT for 24 months
2	LUL	1.0×1.0	0.82[a]	0.82[a]	Resolved spontaneously
3	RUL	1.4×1.1	2.50	3.93	Stable on CT for 24 months
4	RUL	1.0×0.8	1.39	3.54	Small cell lung cancer
5	RUL	0.8×0.8	2.16	10.22	Non-small cell lung cancer
6	RUL	1.0×1.0	1.08	3.01	Adenocarcinoma
7	R apex	1.2×1.2	1.48	6.91	Moderately differentiated adenocarcinoma
8	RML	0.9×0.9	0.63[a]	0.63[a]	Stable on CT for 25 months
9	RLL	1.5×1.0	1.84	3.48	Well-differentiated adenocarcinoma
10	LUL	1.5×1.5	6.04	10.82	Moderately differentiated adenocarcinoma
11	LUL	1.5×1.5	0.88[a]	0.88[a]	Decreased size on CT done 4 mo. later
12	RUL	1.7×1.4	5.20	6.18	Breast cancer metastasis
13	LUL	1.7×1.6	0.74[a]	0.74[a]	Bronchioalveolar carcinoma
14	RLL	1.8×1.0	1.63	3.76	Moderately differentiated adenocarcinoma
15	RUL	1.8×1.8	4.49	5.95	Breast cancer metastasis
16	LUL	1.9×1.1	2.91	3.96	Squamous cell carcinoma
17	RUL	1.9×1.2	5.24	8.89	Squamous cell carcinoma
18	LUL	2.0×2.0	2.21	2.56	Lymphoma
19	LUL	2.0×2.0	2.74	2.57	Granuloma
20	LUL	2.0×2.0	2.49	2.90	Poorly differentiated squamous carcinoma
21	RUL	2.0×1.8	5.71	6.28	Bronchioalveolar carcinoma
22	RLL	2.0×1.8	2.61	4.11	Malignant
23	LUL	2.0×2.0	4.10	6.41	Poorly differentiated adenocarcinoma
24	RML	2.0×2.0	2.16	2.68	Resolved spontaneously
25	RLL	0.8×0.8	0.83[a]	0.83[a]	Stable on CT for 24 months
26	LLL	2.2×2.2	1.01[a]	1.01[a]	Hamartoma
27	RML	2.2×2.0	4.37	4.89	Carcinoid
28	R apex	2.5×2.0	6.99	4.30	Non-small cell lung cancer
29	RUL	2.5×2.5	3.35	5.71	Adenocarcinoma
30	LUL	2.5×1.5	4.45	7.73	Malignant
31	RUL	2.5×2.5	10.49	9.98	Poorly differentiated squamous carcinoma
32	LUL	3.0×2.6	4.24	4.09	Poorly differentiated adenocarcinoma
33	LUL	2.7×1.5	2.69	3.79	Poorly differentiated adenocarcinoma
34	RUL	2.9×2.9	7.26	5.51	Poorly differentiated adenocarcinoma
35	RUL	3.0×3.0	4.59	3.67	Non-small cell lung cancer
36	RUL	3.0×1.6	4.84	4.48	Well-differentiated adenocarcinoma
37	RLL	3.0×1.5	4.37	8.06	Non-small cell lung cancer
38	RUL	3.0×3.0	11.89	8.73	Adenocarcinoma
39	RUL	3.0×2.5	7.26	10.63	Adenocarcinoma
40	LLL	3.4×2.8	5.95	4.39	Adenocarcinoma
41	RUL	3.9×2.3	4.96	4.97	Non-small cell lung cancer
42	LLL	4.0×3.5	16.57	7.96	Non-small cell lung cancer
43	RLL	4.2×4.2	5.62	2.92	Adenocarcinoma
44	RLL	5.0×4.5	7.93	4.85	Non-small cell lung cancer
45	RLL	2.2×2.0	2.21	2.93	Adenocarcinoma
46	LUL	0.9×0.9	0.99[a]	0.99[a]	Stable on CT for 28 months
47	RUL	0.5×0.5	1.33[a]	1.33[a]	Stable on CT for 28 months

LUL, left upper lobe; RUL, right upper lobe; LLL, left lower lobe; RLL, right lower lobe; RML, right middle lobe; R apex, right apex

[a] These could not be identified by increased FDG uptake. A background region of interest in the approximate location on CT was used instead to determine both the maxSUV and the corSUV

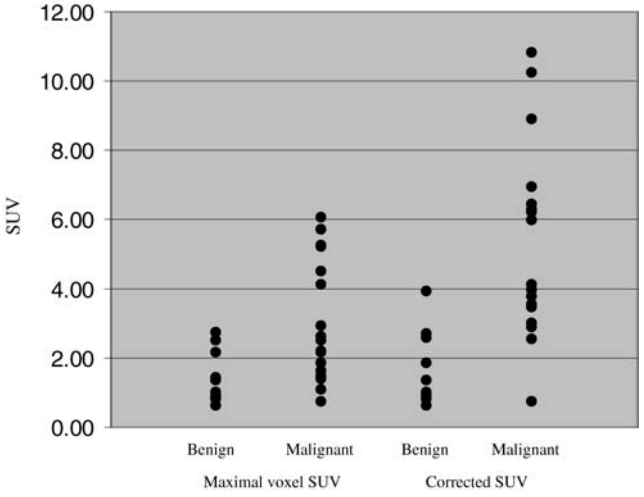

Fig. 3. SUVs of benign and malignant lung lesions measuring equal to or less than 2 cm using both methods

phantom with 9,293 ml of radiolabeled saline containing 74.0 MBq (2.0 mCi) of ^{18}F [12].

For lesions that could not be clearly identified by increased FDG uptake, an ROI of background in the approximate lesion's location on CT was used instead to determine both the maxSUV and the corSUV.

Table 2. Sensitivity, specificity, and accuracy for characterization of lung lesions measuring up to 2.0 cm in maximal diameter for different SUV cutoff values using the maxSUV

SUV	TP	TN	FN	FP	Sens. (%)	Spec. (%)	Acc. (%)
1.0	16	4	1	6	94	40	74
1.5	12	7	5	3	71	70	70
2.0	11	7	6	3	65	70	67
2.5	8	8	9	2	47	80	59
3.0	6	10	11	0	35	100	59

Table 3. Sensitivity, specificity, and accuracy for characterization of lung lesions measuring up to 2.0 cm in maximal diameter for different SUVcutoff values using the corSUV

SUV	TP	TN	FN	FP	Sens. (%)	Spec. (%)	Acc. (%)
1.0	16	3	1	7	94	40	70
1.5	16	6	1	4	94	60	81
2.0	16	7	1	3	94	70	85
2.5	16	7	1	3	94	70	85
3.0	14	9	3	1	82	90	85

Results

Of the 47 lung lesions evaluated, 36 were malignant and 11 were benign. The diagnosis of benignity was based on the stability of the lesion on follow-up CT scans in 10 patients and on the results of excisional biopsy in one. All malignant lesions were confirmed by biopsy.

Among small lesions, 17 were malignant and 10 were benign. Using the maximal voxel SUV to characterize these lesions, the mean SUV was 1.43±0.77 and 3.02±1.74 for benign and malignant lesions respectively (Fig. 3; Table 1). For the initial analysis of the data, an SUV below 2.5 was considered to represent a benign process. Based on this criterion, there were eight true positives (TP), eight true negatives (TN), nine false negatives (FN) and two false positives (FP), giving an overall sensitivity, specificity, and accuracy of 47%, 80%, and 59% respectively. On this study, the sensitivity is defined as the probability of a malignant lesion having a correct diagnosis. The specificity is defined as the probability of a benign lesion being correctly interpreted as not malignant. The accuracy is the probability of all lesions being correctly interpreted as malignant or benign. When an SUV of 2.0 was used for cutoff, there were 11 TP, 7 TN, 6 FN, and 3 FP, giving a sensitivity, specificity, and accuracy of 65%, 70% and 67% respectively. When all lesions with no increased FDG uptake were excluded, the sensitivity, specificity, and accuracy were 69%, 25%, and 60%, respectively, for an SUV threshold of 2.0 and 50%, 50%, and 50%, respectively, for a threshold of 2.5. Using an SUV corrected for partial volume effect, the mean SUV was 1.65±1.09 for benign lesions and 5.28±2.71 for malignant lesions. There were 16 TP, 7 TN, 1 FN, and 3 FP, giving a sensitivity of 94%, a specificity of 70%, and an accuracy of 85% when an SUV of either 2.0 or 2.5 was used as the cutoff. When all lesions with no increased FDG uptake were excluded, the sensitivity, specificity, and accuracy were 100%, 25%, and 85%, respectively, for an SUV threshold of 2.0 or 2.5. The sensitivities and specificities for diagnosing malignant lesions and the accuracy were calculated for other SUV cutoff values using the maxSUV (Table 2) and corSUV (Table 3) methods. These values were also determined for both SUV methods when all lesions with no increased FDG uptake were excluded (Tables 4 and 5).

Among large lesions, 19 were malignant and 1 was benign. Using the maxSUV, the mean SUV was 1.01±1.01 and 6.32±3.50 for benign and malignant lesions respectively (Fig. 4; Table 1). There were 19 TP, 1 TN, 0 FN and 0 FP, giving an overall sensitivity and accuracy of 100% when the SUV of 2.0 was used for cutoff to distinguish benignity from malignancy. When an SUV cutoff of 2.5 was used, there were 18 TP, 1 TN, 1 FN and 0 FP, which resulted in a sensitivity and accuracy of 95% for both. Using the SUV corrected for resolution effect, the mean SUV was 1.01±1.01 for benign lesions and 5.95±2.57 for malignant lesions. There were 19 TP, 1 TN, 0 FP and 0 FN, giving a sensitivity and accuracy

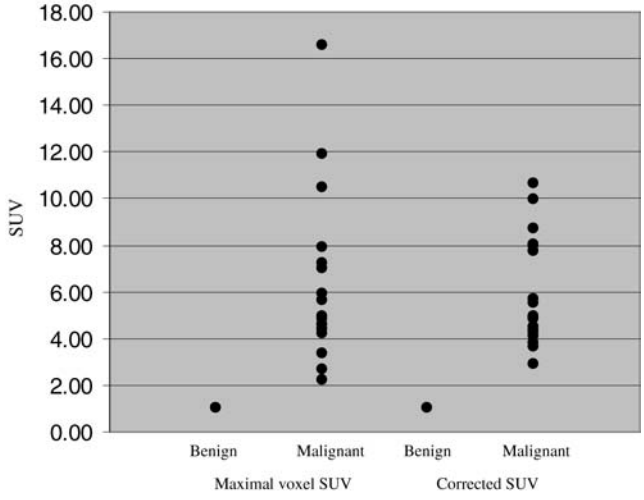

Fig. 4. SUVs of benign and malignant lung lesions measuring more than 2 cm using both methods

Table 4. Sensitivity, specificity, and accuracy for characterization of lung lesions with increased FDG uptake and measuring up to 2.0 cm in the maximal diameter for different SUV cutoff values using the maxSUV

SUV	TP	TN	FN	FP	Sens. (%)	Spec. (%)	Acc. (%)
1.0	16	0	0	4	100	0	80
1.5	13	1	3	3	81	25	70
2.0	11	1	5	3	69	25	60
2.5	8	2	8	2	50	50	50
3.0	5	4	11	0	19	100	45

Table 5. Sensitivity, specificity, and accuracy for characterization of lung lesions with increased FDG uptake and measuring up to 2.0 cm in the maximal diameter for different SUV cutoff values using the corSUV

SUV	TP	TN	FN	FP	Sens. (%)	Spec. (%)	Acc. (%)
1.0	16	0	0	4	100	0	80
1.5	16	0	0	4	100	0	80
2.0	16	1	0	3	100	25	85
2.5	16	1	0	3	100	25	85
3.0	14	3	2	1	88	75	85

both equaling 100% whether the SUV of 2.0 or 2.5 was used as cutoff.

Discussion

PET imaging with FDG has been proven to be a useful diagnostic modality in differentiating benign from malignant lung lesions. Sensitivity, specificity, and accuracy in the ranges of 82%–100%, 60%–100%, and 79%–100%, respectively, have been reported in the literature [13, 14, 15]. However, FDG is not a tumor-specific tracer. Multiple infectious or inflammatory processes, including tuberculosis [16, 17], *Mycobacterium avium-intracellulare* infection[18], invasive aspergillosis [19], abscess [14], and chondrohamartomas [8], can have increased FDG uptake and potentially cause false positive results. It is not surprising that in our study, we noted a lung nodule that was eventually proven to be a granuloma and met the criteria for malignancy with both SUV measurement methods.

On the other hand, there are three major settings in which false negative FDG-PET studies may occur: small lesion size, low tumor metabolic activity, and hyperglycemia [6, 20]. Investigators from different groups have tried to reduce potential false positive and false negative interpretations of FDG-PET. First, different value of SUV have been established to distinguish malignant from benign lesions [3, 21]. However, it appears that too many factors can affect the level of SUV and therefore a diagnosis purely based on SUV level might not be accurate enough. Secondly, based on the observation that inflammatory and malignant cells exhibit a differential FDG uptake pattern over time [22], it has been proposed that delayed image or dual-time point imaging might be used to separate malignant from benign lesions [23, 24, 25]. However, not all malignant lesions exhibit increasing FDG uptake and some benign lesions, such as sarcoidosis, may also demonstrate increasing FDG uptake over time [25]. Therefore, other methods to further improve the accuracy of FDG-PET are needed in this setting.

The accuracy of characterization of lung nodules as malignant is well known to be affected by lesion size. A slightly lower sensitivity has been reported for nodules measuring less than 1.5 cm in diameter [26]. Our study demonstrated that PET imaging was accurate in characterizing lung lesions measuring more than 2 cm using the standard SUV measurement at the voxel with maximal activity. However, the accuracy for small lesions measuring 2 cm or less was significantly lower. This is very likely attributable to partial volume effects due to the limited resolution of PET imaging and patient motion during examination. This can lead to a considerable underestimation of the true activity concentration within lesions with a diameter of less than twice the resolution of the PET scanner at full-width at half-maximum (FWHM). The resolution of our scanner is 4.6 mm at FWHM using phantoms [12]. The actual spatial resolution is worse considering the respiratory motion, scatter, and noise. For these reasons, a diameter of 2.0 cm on CT scan was used as a threshold to subdivide lung lesions into small or large and to determine whether correction for partial volume effect using either CT or PET can result in accurate estimation of SUV for differentiation of benign from malignant nodules.

A potentially more accurate method to correct the SUV for partial volume effect is to determine the volume of the lesion on CT scan and the number of counts throughout the entire volume of perceived increased FDG uptake, and to correct for background. Unfortunately, this method is very cumbersome and time-consuming. Imaging of these nodules with thin slices with a high-resolution CT scanner is needed for accurate volume determination. The lung nodules are imaged with a helical CT scan using usually a slice thickness and pitch of 7 mm. For this reason, an accurate measurement can be determined only in the transaxial plane and not in the longitudinal axis.

A reasonable compromise is to utilize the proposed method in only one plane on the transaxial images of the PET study demonstrating maximal lesional activity and on the CT scan with maximal lesional size. This method is accurate for lesions with a relatively uniform count density. One potential shortcoming is that the CT slice of maximal surface area may not match with the image that contains the maximum count density on FDG-PET. In small lung nodules, which measure 2 cm or less in greatest diameter, the number of slices usually spans up to three or four on CT images using a conventional slice thickness and pitch both of 7 mm. The vast majority of these small lesions are relatively spherical or ovoid in shape. This indicates that the surface area of the peripheral slices of the lesion is less than that of the inner one or two slices in the transaxial planes. In these peripheral slices, the perceived count density is more decreased due to the partial volume effect as compared with that of the inner slices. In addition, this method for the calculation of the SUV is not expected to be of value for lesions with central necrosis. This is most often seen in large lesions that have outgrown their blood supply and is uncommon in small lesions. For these reasons, the potential for misregistration of the maximum count density on FDG-PET with the largest slice on CT scan is low in the case of small lesions. Another potential shortcoming lies in the determination of the background activity. We adopted a perilesional region for background to obtain a maximally reproducible result. Unfortunately, the background activity is potentially overestimated in lesions adjacent to structures with relatively intense FDG activity such as the heart, mediastinal structures, and the chest wall. Despite this limitation, we obtained a high accuracy with this method for the characterization of small lung nodules.

By adopting SUV measurements, which are corrected for resolution effect, the accuracy of characterization of small lesions was improved significantly as compared with that achieved using the maximal SUV calculations, which are based on maximal voxel activity. By adopting the former, and compared with the latter, the sensitivity, specificity and accuracy improved from 65%, 70%, and 67% respectively to 94%, 70%, and 85% respectively when the SUV of 2.0 was used as a cutoff to differentiate benignity from malignancy. Figure 2 illustrates an example of a small lesion with FDG uptake somewhat higher than that of background, and having a substantial increase in the calculated SUV with the use of the corSUV method as compared with the value obtained using the maxSUV method. For large lesions, the proposed technique for measuring the SUV did not improve the accuracy. In fact, the SUV measurements for large malignant lung lesions using the corSUV method were not significantly different from the values generated by the maxSUV method. Large lung lesions, particularly those with necrotic centers, often demonstrate heterogeneous FDG uptake, which explains the relative underestimation of the corSUV as compared with the maxSUV, observed in Table 1. Therefore for small lung nodules, by combining the anatomic data from CT with the metabolic measurements provided by PET, we were able to develop one accurate method of measuring the SUV. This method, however, did not improve the already very high accuracy achieved using the maxSUV method in our population with large lung lesions.

Another method that can be potentially valuable in distinguishing benign from malignant lung nodules is dual-time point imaging. Zhuang et al. have demonstrated that cancerous lesions demonstrate increasing FDG activity over time [24]. The SUV increased on average by 19% between the first and second scans taken at approximately 45 and 90 min respectively. By contrast, the SUV of benign lung nodules remained relatively stable over time, with a modest average SUV decrease of 6% between the first and second scans. One possible reason for this difference in the pattern of FDG uptake over time is that cancerous lesions have on average lower glucose-6-phosphatase activity than benign lesions. With this technique, a second emission scan of a small region centered at the level of the nodule would be required at the end of the study. Although applying the dual-time point will prolong the duration of the FDG-PET examination by 14–15 min, this technique appears to be useful to improve the accuracy of the characterization of lung nodules with an SUV value close to the threshold of 2.5. Plans are also underway to combine these two techniques to further improve the performance of the FDG-PET technique in characterizing lung nodules.

Hyperglycemia is also known to result in decreased FDG uptake in malignant lesions [27, 28, 29]. This is partially attributed to competitive inhibition of FDG uptake by high serum glucose concentrations. Research has shown that the inhibitory effect is most significant in rapid onset hyperglycemia while chronically elevated glucose levels only minimally affect FDG uptake by tumors (reducing it by approximately 10%) [30]. Interestingly, Nakamoto et al. reported a slightly more reproducible value by multiplying the SUV by the plasma glucose concentration [31].

Our study also revealed a lack of increased FDG uptake in a bronchioalveolar carcinoma (BAC). Several

factors may account for the lack of FDG uptake in this malignancy. It may be partly due to a low metabolic demand for glucose or to the relatively sparse presence of metabolically active malignant cells in this generally slow-growing tumor [32]. Glucose metabolism measured by FDG-PET correlates with tumor growth in lung cancer [33, 34]. Fortunately, BAC is associated with an overall survival that is significantly longer than that of non-BAC lung carcinomas [35]. It has also been reported that low tumor FDG uptake is associated with longer survival than that observed with high tumor metabolic activity [36].

One limitation of our study is the small number of confirmed benign lung lesions. Lung nodules that meet the FDG-PET criteria for malignancy are biopsied and/or excised shortly after the study. Thus, histological confirmation is readily available for these lesions. Bronchoscopic or transthoracic needle biopsy is associated with significant morbidity and does not definitively exclude malignancy owing to the potential inadequacy of samples [8]. One study reported a 19% FN rate for malignancy and a 25%–56% risk of pneumothorax [37]. Based on the data published in the literature, benign lung lesions that do not meet the criteria for malignancy on FDG-PET are rarely biopsied and are monitored using a repeat CT scan several months later. However, the uncertainty of the nature of the lesion and other factors require an approach that improves the sensitivity of the technique. Several factors have been associated with an increased pretest probability of malignancy in lung nodules: patient's age, nodule size, appearance of the nodule on CT scan and the patient's smoking habits [15]. Absence of these risk factors supports conservative management that includes follow up CT scan at regular intervals and obviates the need for invasive biopsy procedures, particularly in patients who are poor candidates for surgical intervention [26].

The criteria for benignity that we used were standard, i.e. excisional biopsy with histological confirmation or serial CT scans demonstrating stability of the lesion's size over a minimum period of 24 months or a spontaneous decrease in lesion size. All patients with lung lesions considered benign on the study were free of malignancy on follow-up observation. Among the 11 benign lesions that did not meet our criteria for malignancy, none increased in size on CT scan and none developed clinical manifestation of malignancy. Amongst the three false positive results, one was an active granuloma, one remained stable in size for 24 months on CT scan and the other resolved spontaneously as shown by follow-up CT scan performed 6 months later. The last-mentioned was a 2-cm lesion demonstrating moderately increased uptake with a maxSUV of 2.16 and a corSUV of 2.68. This was our only case in which applying the SUV using the size determined on CT scan to calculate the SUV resulted in a false positive result when the SUV of 2.5 was used for cutoff.

In conclusion, measuring the SUV by using the CT size to correct for resolution effect offers potential value in distinguishing malignant from benign lesions in this population. This semiquantitative approach appears to improve considerably the sensitivity and accuracy in characterizing malignant small lung nodules in this population. Further studies are suggested to confirm these preliminary results and to determine the reproducibility of these data in a large population with solitary pulmonary nodules.

References

1. Mori K, Saitou Y, Tominaga K, et al. Small nodular lesions in the lung periphery – new approach to diagnosis with CT. *Radiology* 1990; 177:843–849.
2. Lowe VJ, Hoffman JM, DeLong DM, Patz EF, Coleman RE. Semiquantitative and visual analysis of FDG-PET images in pulmonary abnormalities. *J Nucl Med* 1994; 35:1771–1776.
3. Patz EF Jr, Lowe VJ, Hoffman JM, et al. Focal pulmonary abnormalities: evaluation with F-18 fluorodeoxyglucose PET scanning. *Radiology* 1993; 188:487-490.
4. Al-Sugair A, Coleman RE. Applications of PET in lung cancer. *Semin Nucl Med* 1998; 28:303-319.
5. Delbeke D, Sandler MP. The role of hybrid cameras in oncology. *Semin Nucl Med* 2000; 30:268–280.
6. Bar-Shalom R, Valdivia AY, Blaufox MD. PET imaging in oncology. *Semin Nucl Med* 2000; 30:150–185.
7. Duhaylongsod FG, Lowe VJ, Patz EF Jr, Vaughn AL, Coleman RE, Wolfe WG. Detection of primary and recurrent lung cancer by means of F-18 fluorodeoxyglucose positron emission tomography (FDG PET). *J Thorac Cardiovasc Surg* 1995; 110:130–139; discussion 139–140.
8. Prauer HW, Weber WA, Romer W, Treumann T, Ziegler SI, Schwaiger M. Controlled prospective study of positron emission tomography using the glucose analogue F-18 fluorodeoxyglucose in the evaluation of pulmonary nodules. *Br J Surg* 1998; 85:1506-1511.
9. Weber W, Young C, Abdel-Dayem HM, et al. Assessment of pulmonary lesions with F-18-fluorodeoxyglucose positron imaging using coincidence mode gamma cameras. *J Nucl Med* 1999; 40:574–578.
10. Daube-Witherspoon ME, Matej S, Karp JS, Lewitt RM. Application of the row action maximum likelihood algorithm with spherical basis functions to clinical PET imaging. *IEEE Trans Nucl Sci* 2001; 48:24–30.
11. Browne J, DePierro AR. A row-action alternative to the EM algorithm for maximizing likelihoods in emission tomography. *IEEE Trans Med Imaging* 1996; 15:687–699.
12. Adam LE, Karp JS, Daube-Witherspoon ME, Smith RJ. Performance of a whole-body PET scanner using curve-plate NaI(Tl) detectors. *J Nucl Med* 2001; 42:1821–1830.
13. Slosman DO, Spiliopoulos A, Couson F, et al. Satellite PET and lung cancer: a prospective study in surgical patients. *Nucl Med Commun* 1993; 14:955–961.
14. Hubner KF, Buonocore E, Singh SK, Gould HR, Cotten DW. Characterization of chest masses by FDG positron emission tomography. *Clin Nucl Med* 1995; 20:293–298.
15. Gupta NC, Maloof J, Gunel E. Probability of malignancy in solitary pulmonary nodules using fluorine-18-FDG and PET [see comments]. *J Nucl Med* 1996; 37:943–948.

16. Cook GJ, Fogelman I, Maisey MN. Normal physiological and benign pathological variants of 18-fluoro-2-deoxyglucose positron-emission tomography scanning: potential for error in interpretation. *Semin Nucl Med* 1996; 26:308–314.
17. Bakheet SMB, Powe J, Ezzat A, Rostom A. F-18-FDG uptake in tuberculosis. *Clin Nucl Med* 1998; 23:739.
18. Zhuang HM, Pourdehnad M, Yamamoto AJ, Rossman MD, Alavi A. Intense F-18 fluorodeoxyglucose uptake caused by *Mycobacterium avium intracellulare* infection. *Clin Nucl Med* 2001; 26:458.
19. Ozsahin H, von Planta M, Muller I, et al. Successful treatment of invasive aspergillosis in chronic granulomatous disease by bone marrow transplantation, granulocyte colony-stimulating factor-mobilized granulocytes, and liposomal amphotericin-B. *Blood* 1998; 92:2719.
20. Lowe VJ, Naunheim KS. Positron emission tomography in lung cancer. *Ann Thorac Surg* 1998; 65:1821–1829.
21. Hubner KF, Buonocore E, Gould HR, et al. Differentiating benign from malignant lung lesions using "quantitative" parameters of FDG PET images. *Clin Nucl Med* 1996; 21:941–949.
22. Yamada S, Kubota K, Kubota R, Ido T, Tamahashi N. High accumulation of fluorine-18-fluorodeoxyglucose in turpentine-induced inflammatory tissue. *J Nucl Med* 1995; 36:1301–1306.
23. Boerner AR, Weckesser M, Herzog H, et al. Optimal scan time for fluorine-18 fluorodeoxyglucose positron emission tomography in breast cancer. *Eur J Nucl Med* 1999; 26:226–230.
24. Zhuang HM, Pourdehnad M, Lambright ES, et al. Dual time point F-18-FDG PET imaging for differentiating malignant from inflammatory processes. *J Nucl Med* 2001; 42:1412–1417.
25. Kubota K, Itoh M, Ozaki K, et al. Advantage of delayed whole-body FDG-PET imaging for tumour detection. *Eur J Nucl Med* 2001; 28:696–703.
26. Dewan NA, Shehan CJ, Reeb SD, Gobar LS, Scott WJ, Ryschon K. Likelihood of malignancy in a solitary pulmonary nodule: comparison of Bayesian analysis and results of FDG-PET scan. *Chest* 1997; 112:416–422.
27. Langen KJ, Braun U, Rota Kops E, et al. The influence of plasma glucose levels on fluorine-18-fluorodeoxyglucose uptake in bronchial carcinomas. *J Nucl Med* 1993; 34:355–359.
28. Lowe VJ, Delong DM, Hoffman JM, Coleman RE. Optimum scanning protocol for FDG-PET evaluation of pulmonary malignancy. *J Nucl Med* 1995; 36:883–887.
29. Zhuang HM, Cortes-Blanco A, Pourdehnad M, et al. Do high glucose levels have differential effect on FDG uptake in inflammatory and malignant disorders? *Nucl Med Commun* 2001; 22:1123–1128.
30. Torizuka T, Clavo AC, Wahl RL. Effect of hyperglycemia on in vitro tumor uptake of tritiated FDG, thymidine, L-methionine and L-leucine. *J Nucl Med* 1997; 38:382.
31. Nakamoto Y, Zasadny KR, Heikki M, Wahl RL. Reproducibility of common semi-quantitative parameters for evaluating lung glucose metabolism with positron emission tomography using 2-deoxy-2-[^{18}F]fluoro-D-glucose. *Mol Imag Biol* 2002; 4:171–178.
32. Higashi K, Ueda Y, Seki H, et al. Fluorine-18-FDG PET imaging is negative in bronchioloalveolar lung carcinoma. *J Nucl Med* 1998; 39:1016–1020.
33. Duhaylongsod FG, Lowe VJ, Patz EF Jr, Vaughn AL, Coleman RE, Wolfe WG. Lung tumor growth correlates with glucose metabolism measured by fluoride-18 fluorodeoxyglucose positron emission tomography. *Ann Thorac Surg* 1995; 60: 1348–1352.
34. Higashi K, Ueda Y, Yagishita M, et al. FDG PET measurement of the proliferative potential of non-small cell lung cancer. *J Nucl Med* 2000; 41:85–92.
35. Okubo K, Mark EJ, Flieder D, et al. Bronchoalveolar carcinoma: clinical, radiologic, and pathologic factors and survival. *J Thorac Cardiovasc Surg* 1999; 118:702–709.
36. Vansteenkiste JF, Stroobants SG, Dupont PJ, et al. Prognostic importance of the standardized uptake value on F-18-fluoro-2-deoxy-glucose-positron emission tomography scan in non-small-cell lung cancer: an analysis of 125 cases. *J Clin Oncol* 1999; 17:3201.
37. Dewan N, Reeb S, Gupta N, Gobar L, Scott W. PET FDG imaging and transthoracic needle lung aspiration biopsy in evaluation of pulmonary lesions. *Chest* 1995; 108:441–446.